Energy Engineering and Management, Vol. 13, No. 4, PP. 36-47, 2024

Effect of Annular Injector Geometry and Different Injection Functions on Diesel Engine Performance: A Numerical Study

Rasool Esmaelnajad[1*], Navid Farrokhi[2]

[1] Miyaneh Technical and Engineering Faculty, University of Tabriz, Iran
rasool_ra@tabrizu.ac.ir
[2] Department of Mechanical Engineering, Parand Branch, Islamic Azad University, Parand, Iran
n.farrokhi@iau.ac.ir

Keywords:
annular injector,
injection function,
numerical method,
SFC,
diesel engine performance.

Original Research Article

Paper History:
Received: 09/05/2024
Revised: 19/06/2024
Accepted: 22/06/2024
Available online: 25/06/2024

Abstract: Changing the injector orifice geometry has major impact on diesel engine performance. In this study, the geometry of the injector outlet is changed from circular to annular, and the effect of different injection functions on the performance of the diesel engine is investigated. The results are compared with the results of the Kubota 3300 engine. Numerical simulations are conducted by using AVL Fire commercial code. The results show that the annular injector provides a better fuel distribution inside the combustion chamber of the engine by increasing the fuel angle. The use of changing fuel injection rates in the annular injector also improves engine performance. The best performance is observed for the constant-increasing function, and the specific fuel consumption value reached 0.1865. By applying new injection functions as well as by using the new presented annular injector, power also increases. As an instance, for a constant-increasing function (fourth function), despite a decrease in the amount of fuel injection per engine cycle by 8.8%, power increases by 13.6% and 13.5% respectively. While NO pollutant increases slightly by changing the type of the injector and by using spray functions, the soot produced at the beginning of the combustion process is well oxidized before the end of the power stroke, and its amount reaches less than 2e-6.

How to cite this article: Esmaelnajad, R., Farrokhi, N., "*Effect of Annular Injector Geometry and Different Injection Functions on Diesel Engine Performance: A Numerical Study*", Energy Engineering and Management, Vol. 13, No. 4, PP. 36-47, 2024. https://doi.org/10.22052/eem.2024.254617.1063

1. Introduction

One of the efficient methods in improving engine performance and reducing combustion pollutants is improving the fuel spray behavior by changing the injector geometry and controlling its sprayed mass [1-3]. Defining any method and path to achieve performance improvement in diesel engines leads to changes in other combustion parameters. Thus, the combustion factors and the effective pollution should be carefully considered [4-6]. Using multi-hole injectors improves the performance of injectors, because this type of injectors distributes droplets finer and more evenly inside the cylinder. The use of this type of injectors improves the combustion performance of the engine and reduces the amount of the produced pollutants. Compared to single-hole injectors, the droplets are more evenly distributed inside the cylinder, but there are still poor and rich areas in the spray of this type of injectors. Many numerical and experimental studies have been conducted in this field [7-10]. When the fuel hits the combustion chamber surface at high speeds, the distribution of fuel in the combustion chamber and mixing with the air will be weakened, which reduces the amount of air infiltrated into the fuel spray. This increases the soot. Optimal mode for combustion process design is a mode, in which both the amount of fuel spray evaporation and its penetration depth are desirable. For this reason, the diameter of the injector hole is also a key parameter in the performance of the diesel engine. Large diameters increase the diameter of the droplets as well as the penetration length, while small diameters reduce sprayed mass and penetration length [11-12]. The use of square, triangular, elliptical, and rectangular sections at high pressures for fuel spraying has been considered in recent years. The results show that flat injectors (elliptical and rectangular) have better spray angle, and fuel is powdered faster in them [13-16]. The annular section geometry also has a flat fuel outlet, and thus has the characteristics of flat non-circular sections. Therefore, annular cross-section and its resulting spray have been studied in recent years. Migliko et al. [17] investigated the behavior of fuel sprayed from annular injectors at very high pressures. Based on their results, the spray from annular injector has high spray angle and low penetration length, which can be used to inject large amount of fuel in a short time. Jeon et al. [18] investigated the effects of ambient density on initial flow failure and size distribution of droplets sprayed from circular sections. Based on the results of their work, increasing the ambient density reduces decomposition length of the liquid film, though with increasing initial flow turbulence, the effects are negligible. Size of the spray droplets decreases in the area near the nozzle as the density of the medium increases, but the reverse trend is observed downstream because the atomization of the spray at high density of the medium ends faster. Gao et al. [14] investigated the effect of fuel temperature and ambient pressure and temperature on droplets generated from gasoline by annular injectors. Their results show that while Thesauter mean diameter (SMD) was found to be increased with increasing ambient pressure and fuel injection time, it decreased with increasing fuel temperature. Du et al. [20] investigated effects of charge gas temperature, gas pressure, and fuel type on liquid penetration length and cone angle of an annular spray from a piezoelectric injector. They found that density, specific heat, surface tension, and vaporization heat are the most influential physical properties on spray penetration. Wu et al. [21] experimentally studied influence of ambient pressure on spray characteristics of a self-pressurized injector. They observed a distinct flash-boiling induced vortex-ring inside the spray together with rapid evaporation, which improved the spray dispersion. Gimeno et al. [22] experimentally investigated the effect of varying co-flow conditions, fuel mass flow rate, and fuel type on both the flame lift-off height and soot formation. The fuels were injected through an annular spray injector. The comparison among the fuels used demonstrates that the differences in soot formation are mostly related to the fuels sooting tendency. Soundararajan et al. [23] studied influence of the injection system on combustion instabilities on a laboratory-scale combustor equipped with annular injector. They used their model combined with damping rate estimates to predict oscillation amplitudes. With the development of common rail injectors and the use of electronic control in them, it was possible to create high pressures and different mass functions in the injectors. By changing the spray pressure, the amount of mass entering the cylinder can be changed. Fuel spraying at high pressures generally improves the fuel spray behavior. Also the use of different spray functions improves spraying performance [24-26]. Different fuel mass functions can be used to control engine performance [27-28] such as reducing NO_x and soot pollutants [29]. Different functions are applied in different ways [30]. Due to the fact that deriving a suitable spray function by experimental methods is time consuming and costly, investigating the effect of different spray functions by numerical methods has been considered by many researchers [31-32]. In using different spray functions, spraying is done as single or multiple strategies [33-35]. Today, in order to improve the performance of gasoline engines, various injection functions are used [36-37].

To the best of the authors' knowledge, there have not been many researches investigating the annular injectors. In the present work, an annular cross-section injector with high fuel pressure at the output of the diesel engine injector has been used, and different fuel injection functions have also been used for this type of injectors. Here, it is intended to upgrade the power and improve the performance of the diesel engine by changing the injector geometry and its fuel mass function. For this purpose, an injector with annular outlet section is introduced. This type of injector has an outlet orifice with annular cross-section. The thickness of the cross-section is very small compared to the diameter of the circular injectors, which causes smaller droplets in fuel spray. Six different spray functions are used to change the sprayed mass. The simulations have been conducted using AVL Fire

commercial code. The model studied and the boundary conditions applied are exactly in accordance with the operating conditions of the Kubota 3300 diesel engine.

2. Methodology

Due to the fact that the annular injector outlet is in the form of a sheet, a sheet model is used to simulate the behavior of the spray inside the cylinder. This represents a quasi-experimental model for the primary break-up of the injector outlet sheet. This model is used to determine the initial conditions of the spray such as sheet thickness, break-up velocity and length. Fig.1 shows the model schematic, in which the different parts of the injector as well as the break-up of fuel sheet and the formation of droplets are demonstrated.

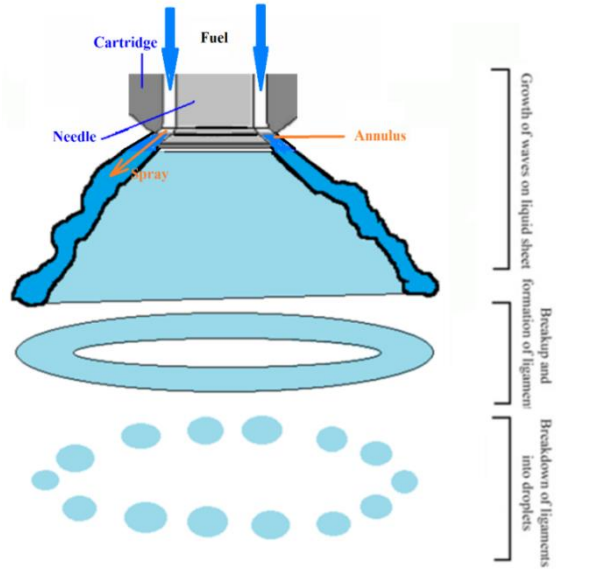

Fig. 1: Sheet breakup model

In this model, fluid film thickness is calculated as [38]:

$$h = \left[\frac{\mathrm{A}\cdot 12\cdot \dot{m_1}\cdot\mu_1}{\pi\cdot\rho_1\cdot d_{out}\Delta p}\cdot\frac{(1+X)}{(1-X)^2}\right]^{0.5} \quad (1)$$

$$X = \frac{(d_{\mathrm{out}}-2\cdot h)^2}{d_{\mathrm{out}}^2} \quad (2)$$

Since h, x are found from equations (1) and (2), an iterative method is used to calculate the thickness.

The K_V velocity coefficient is defined as follows [39]:

$$K_v = \frac{\mathrm{v}}{\left(2\cdot\Delta p/\rho\right)^{0.5}} \quad (3)$$

where K_V is calculated as:

$$K_v = \frac{\mathrm{C_3}}{\cos\theta}\cdot\left(\frac{(1-X)}{1+X}\right)^{0.5} \quad (4)$$

The Clark-Dukowicz relationship is used to calculate the break-up length of the fluid sheet [39].

$$B_L = B\cdot\left[\frac{\rho_l\cdot\sigma\cdot\ln(\frac{\eta}{\eta_0})\cdot\dot{h}\cdot\cos\theta}{\rho_g^2\cdot V_{rel}^2}\right]^{0.5} \quad (5)$$

On the flame front, which is a turbulent flow, reactants (fuel and oxidizer) have the same turbulence intensity that is different from the turbulence intensity of combustion reaction products. According to the turbulent combustion model, chemical reactions have much shorter time scale than the time scale of the turbulence transportation process. It can be assumed that the rate of combustion is determined by the rate of mixing or collision of eddies including reactants and hot products at molecular scale. Therefore, the average reaction rate is expressed as [40].

$$S_{fu} = \overline{\rho\dot{r}} = \frac{\mathrm{C_{fu}}}{\tau_r}\bar{\rho}.min\left(\bar{\mathrm{y}}_{\mathrm{fu}}, \frac{\bar{y}_{Ox}}{S}, \frac{\mathrm{C_{pr}}\bar{y}_{pr}}{1+S}\right) \quad (6)$$

The soot model, used in this study, is based on Hiroyasu polluting pattern [41]. In this model, two physical and chemical processes are used to demonstrate the event of oxidation. Particle formation and surface growth are functions of fuel in a certain place of the combustion chamber and the concentration of soot core in that area respectively. In this model, oxidized soot and the resulting soot are modeled [41]:

$$\frac{dM_{soot}}{dt} = \frac{dM_{form}}{dt} - \frac{dM_{oxide}}{dt} \quad (7)$$

Soot formation is calculated as follows [41]:

$$\frac{dM_{form}}{dt} = \mathrm{A_f}M_{fv}P^{0.5}\exp(-\frac{E_f}{RT}) \quad (8)$$

The soot oxidation rate is calculated according to the following equation [41]:

$$\frac{dM_{oxide}}{dt} = \frac{6MW_c}{\rho_s D_s}M_s R_{tot} \quad (9)$$

The reduction rate of the mixture is determined by the rate of dissolution and the rate of the local turbulent kinetic energy. Nitrogen oxide pattern used in Fire commercial code is the Clark-Dukowicz model [42]. This pattern is highly temperature dependent and is produced by the reaction of nitrogen and oxygen at high temperatures. The concentration of nitrogen oxide has little effect on the flow, and the reaction time of nitrogen oxide is longer than the time interval intended for the mixing process and the combustion. Therefore, the calculations related to nitrogen oxide formation can be separated from the calculations for the main reaction. In this model, the multistage chemical reduction based on the partial equilibrium of the preliminary reactions is as follows:

$$\begin{aligned}&\mathrm{N_2 + O \leftrightarrow NO + N}\\&\mathrm{O_2 + N \leftrightarrow NO + O}\\&\mathrm{N + OH \leftrightarrow NO + H}\end{aligned} \quad (10)$$

The following general reaction is obtained by multiplying the right and left sides of the above equation:

$$N_2 + O_2 \leftrightarrow 2NO \quad (11)$$

Hence, the nitrogen oxide formation rate is extracted according to the following [42]:

$$\frac{d[NO]}{dt} = 2k_f[N_2][O_2] \quad (12)$$

The reaction rate is also derived from the following relation [42]:

$$k_f = \frac{a}{\sqrt{T}} \exp(-\frac{E_a}{RT}) \quad (13)$$

3. Modeling

The investigation of the annular injector behavior under different upstream and downstream conditions is considered. For this purpose, the flow inside the injector must be simulated. The thickness of the injector outlet ring is 0.01 mm, which has an orifice length of 0.5 mm, ring diameter of 2 mm and nozzle outlet with a cone angle of 10°.

The main specifications and operating conditions of the engine used in the current research are given in Table 1. Geometry of the engine used is the same as that of the Kubota 3300 engine, which is a four-stroke direct injection diesel engine with natural aspiration.

Table 1: Engine geometry

Cylinders number	4
Bore (mm)	98
Stroke (mm)	110
Engine volume (L)	3.32

In this study, different injection functions are used to inject fuel into the combustion chamber, which causes the mass of incoming fuel in each cycle to be in 6 different states. The function used for these 6 states is given in Fig. 2. All functions have 20° of spray, and the first function has constant spray rate. This mode is used to compare the effect of using functions in annular injectors compared to a constant spray rate, and its results will also be used to compare the performance of a conventional injector with an annular injector. The quasi-triangular function is used in the second and third injection functions. This type of spraying is widely used in conventional injectors. The fourth function first uses constant mass rate and, then, starts to decrease it after 5°. The sprayed mass first reaches the farthest points of the combustion chamber. With the onset of combustion the spraying rate decreases, which leads to more mixing. The fifth function uses a special form of decreasing-increasing function. The initial spraying is supposed to start combustion; then, by reducing the spraying rate, the ignited mixture is mixed better, and the spraying rate increases. In the sixth function, the mass rate is constant first, but after 5° it starts to increase. In this function, the aim is to start the combustion with a high-oxygen mixture, so that in the next step the fuel is well mixed with the air inside the cylinder using the turbulence created by the movement of the flame front inside the cylinder. However, increasing the mass rate, the penetration length that is controlled by increasing the initial temperature created by the initial combustion increases.

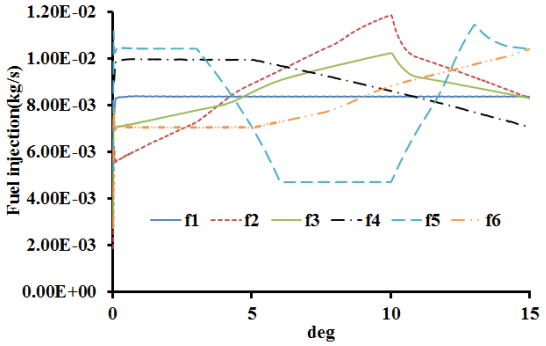

Fig. 2: Mass functions

For solving the governing equations, the computational domain is meshed using hexagonal cells. Grid independency is discussed afterwards. The type of piston crown used in the present work has been slightly changed, because the annular injector sprays to the central region of the cylinder, but multi-hole injectors (used in Kubota engine) perform spraying with a specific angle to the cylinder wall. AVL Fire commercial code was used, and a quarter of the cylinder chamber was modeled and meshed to conduct the simulations. In the present work, the type of fuel and its temperature are constant. The estimated values for the fuel characteristics are given in Table 2.

Table 2: Fuel characteristics

Density (kg/m^3)	Dynamic viscosity (Ns/m^2)	Temperature (K)
830	0.00214	293.15

The internal conditions of the cylinder at the beginning of compression stroke are considered to be constant in all cases. The specifications are given in Table 3.

Table 3: Condition of the cylinder at the beginning of the compression

Temperature (K)	Pressure (kPa)	Air density (kg/m^3)
293	100	1.21

4. Grid Independency

The results of the solution should be independent of the number of the cells. For this purpose, by producing meshes with different cell numbers, the suitable cell number is selected. The basis of the grid independency is the results of the cylinder internal pressure. Four different computational cell numbers were used. The pressure changes versus the crank angle for different cell numbers are shown in Fig. 3.

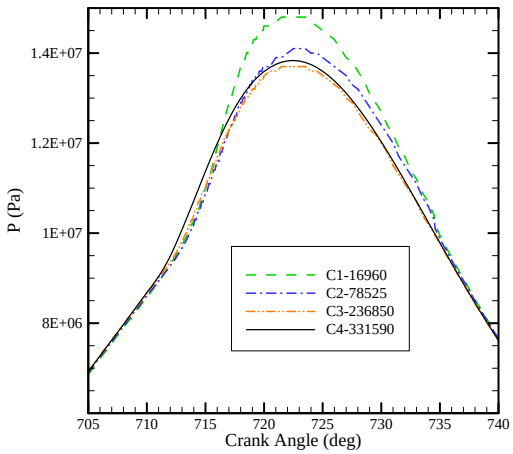

Fig. 3: Pressure variations for different grids

As it can be seen, the pressure variation between the third and the fourth cell numbers are very small. Therefore, further increase in cells does not show a significant change in the results, and meshing with cell number 236850 is used.

5. Numerical Method Validation

Before changing the type of injector in the Kubota engine from a conventional multi-hole injector to an annular injector, the combustion performance of the Kubota 3300 engine was simulated with its conventional injector. The engine was tested and numerically simulated at 2600rpm and a compression ratio of 22.6. Fuel spraying started 20° bTDC and was 36 mg per spray. The results obtained for power, SFC and production of NO and soot pollutants were compared and validated with the experimental results of Hassan et al. [43]; the results of numerical simulation demonstrated acceptable agreement with their results. The results of numerical analysis and experimental tests are given in Table 4 for engine performance and in Figs. 4, 5 for produced pollutants.

Table 4: Comparison of the numerical and experimental results

Parameter	Numerical value	Experimental value
Power (kW)	48.88	47.9
SFC (kg/kWh)	0.244	0.237

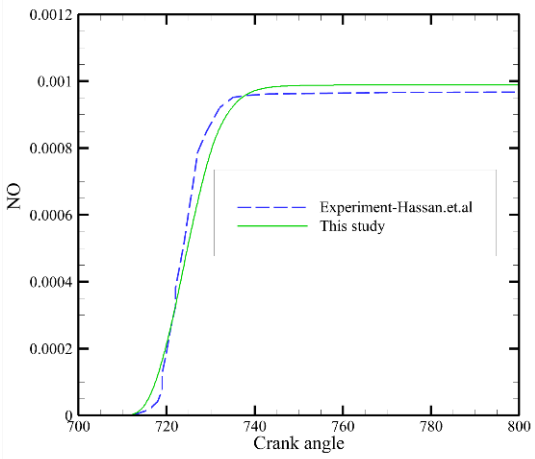

Fig. 4: NO emissions validation

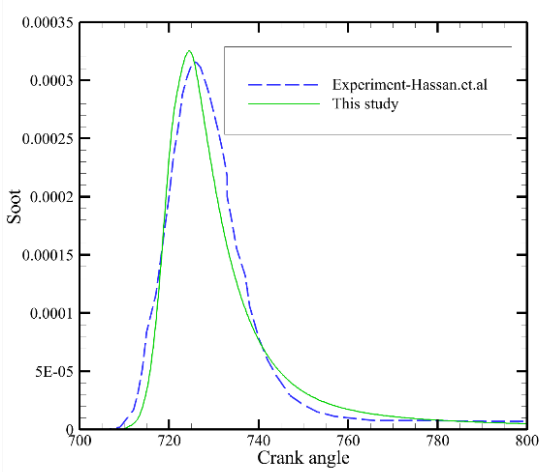

Fig. 5: Soot pollutant validation

6. Results and Discussion

In this study, the effects of annular injectors as well as the effect of different injection functions on engine performance are investigated. The numerical results of the current research were presented in the form of hydrodynamic behavior, fuel spray development pattern, and engine performance parameters as well as the amount of the emissions produced. In this work, the fuel type, compression ratio, and the geometry of the Kubota 3300 engine were kept as constant. The nozzle type was changed from typical six-hole orifice to an orifice with an annular cross-section, and the piston crown shape was changed accordingly.

The mass of fuel entering the combustion chamber in one cycle for the 6 different functions used for fuel injection with the annular injector along with the amount of fuel injection in the Kubota engine are given in Fig. 6. In all spray functions, fuel started from 20° bTDC for as much as 15° of spraying. In order to make comparisons with better conditions, it was tried to avoid very different fuel mass rates for different functions. The highest mass rate was for the fourth function equal to 33.1 mg, and the lowest one was for the sixth function, which was 28.8 mg.

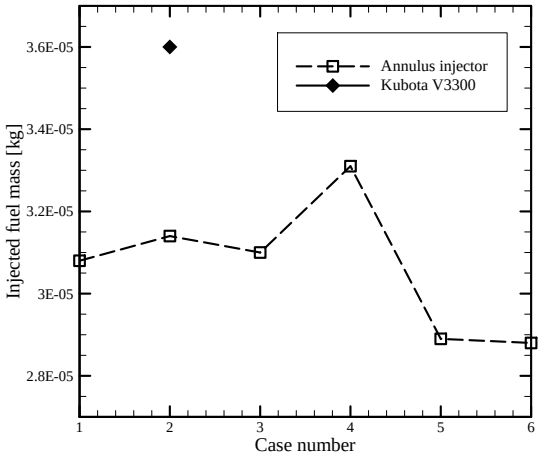

Fig. 6: Variations of fuel mass for different injection patterns

Fig. 7 shows the effect of different spray functions on the pressure inside the combustion chamber, while Fig. 8 demonstrates the temperature in terms of the crankshaft angle from 700° to 760°. Since all the initial conditions of compression stroke were the same for six functions, three factors of combustion efficiency, fuel injection function, and the mass of sprayed fuel will cause different pressures and temperatures for six functions. The higher the combustion efficiency, the better the diesel fuel will burn, resulting in an average temperature and pressure increase. Moreover, a higher fuel mass leads to a higher pressure and temperature inside the combustion chamber. As it can be seen in the last two aforementioned figures, the pressure and temperature behaviors were close to each other. The functions in which the fuel mass was initially high at the time of injection had a higher growth rate, and the the growth trend in the diagrams was directly related to the fuel injection rate. The fourth function had the highest temperature because the fuel mass rate is the highest in this function. The sixth function initially had the lower pressure and temperature than other functions, but after the maximum point, the sixth function no longer had the lowest temperature and pressure, which indicated that combustion had occurred with better timing.

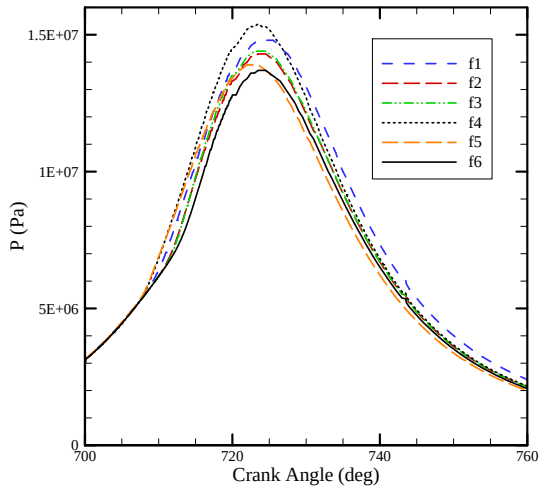

Fig. 7: Pressure variations for different injection patterns

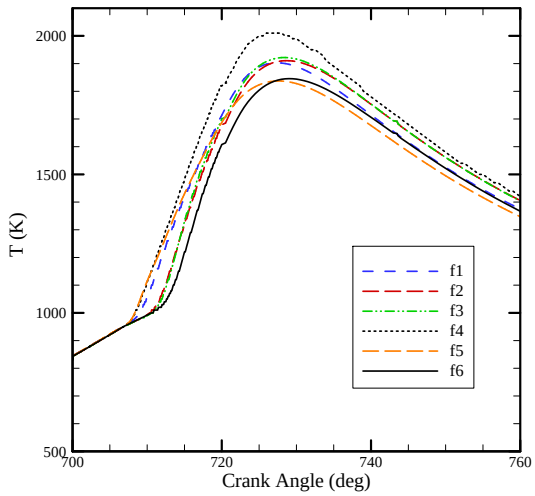

Fig. 8: Temperature variations for different injection patterns

Figs 9, 10 show SFC and power in an engine operating cycle. In these diagrams, the experimental results for the Kubota 3300 engine with a conventional injector are brought together with the numerical results for six sprayed mass functions for an annular injector for comparison. Since in the experimental test of Kubota engine with ordinary injector, a uniform injection function was used, first the experimental results were compared to the results of the first function. By comparing results of the first function with the results presented for the conventional injector, it could be concluded that by changing the injector from the traditional to the annular, performance of the Kubota engine was improved because SFC was reduced by 20%. Also, by changing the type of injector, power increased significantly (taking into account that the sprayed fuel mass had decreased).

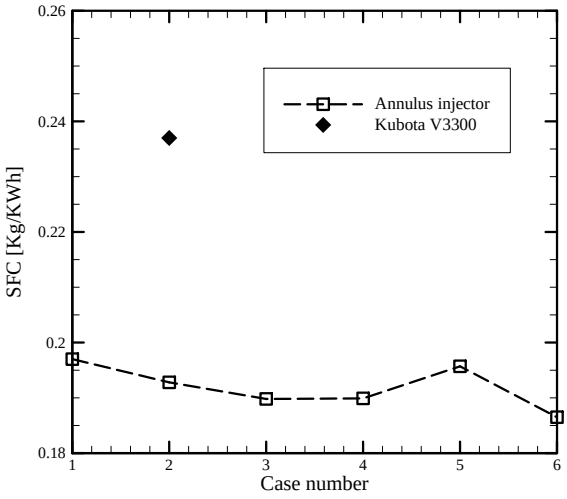

Fig. 9: SFC variations for different injection functions

Fig. 9 also demonstrates SFC changes for six functions under consideration. As it can be seen from the figure, the SFC value for all six annular injector functions was much lower than that for a conventional injector. It can be concluded that the annular injector had improved the fuel injection compared to the conventional injector, which resulted in improved engine combustion performance. Using the spray function improved the performance of the annular injector, which could be concluded from the fact that SFC value for the five spray functions was less than that of the uniform state. Also, from the changes of SFC value for different injection functions, it can be concluded that fuel injection function had great effect on engine performance, which caused a 5% difference between the SFC value for the first and the sixth functions. The third spray function (f3) had a higher performance than the second function (f2). That is, the low-slope quasi-triangular function had a performance higher than the steep-slope mode. The sixth function had the best performance among six provided functions. In cases, where sprayed fuel mass rate was high at the beginning (functions f1 and f2), SFC had higher value, and if sprayed fuel mass rate was low at first (function f6), SFC value was reduced, which indicated further

improvement of engine performance. Since in an injector with annular orifice, the fuel flow rate was higher than a conventional injector, at the beginning of combustion, temperature of the fuel injection area was reduced locally, and also there was not enough opportunity for mixing of the fuel. Therefore, the fuel did not burn completely. However, when the fuel injection flow rate was initially low, the combustion chamber temperature was higher, and its turbulence intensity increased. Also, when the main volume fraction of spray occurred at the end of spraying, it caused the main part of combustion and work to be after TDC. This resulted in an increase in power, which was well illustrated by the pressure distribution diagram.

Comparing the power of the first function with the experimental results of the Kubota engine test in Fig. 10 shows that the sprayed fuel mass had reduced from 36 mg to 30.8 mg, which demonstrated a decrease by 17%. This was while power has increased from 47.9 kW to 48.7 kW. Therefore, using an annular injector in the Kubota 3300 engine, instead of a conventional injector, increases power and improves the performance of the engine as well.

A comparison of six spray functions with each other in the diagram of Fig. 10 shows that the two factors of the sprayed mass and the improvement of the combustion process have caused difference between the values of power of six functions. The power produced with the fourth function had the highest value, because this function had the highest sprayed fuel mass and good combustion performance (only the sixth function has SFC less than this function). In the fourth function, although fuel injection per engine cycle was decreased by 8.8%, power was increased. The increase in power for this type of injection function, compared to Kubota engine, was 13.6% and 13.5% respectively. The fifth function had the lowest amount of power because the sprayed fuel mass was the lowest in this spray function, and the combustion performance of this function was weaker than the other functions (only the first function has higher SFC value).

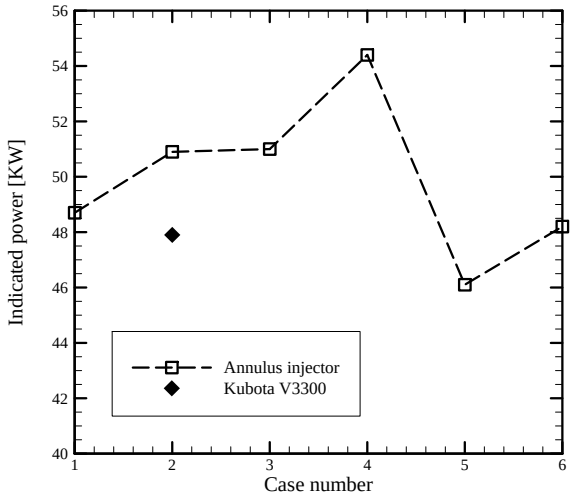

Fig. 10: Power variations for different injection functions

With the beginning of combustion and an increase in the temperature inside the cylinder, nitrogen began to decompose at high temperature points, and NO production increased. Nitrogen oxide changes for six different functions studied in this work were demonstrated in Fig. 11. This pollutant reached a constant value after a few degrees aTDC, because all the fuel burns and the high temperature points disappear. Also, after TDC the combustion chamber began to expand, which resulted in a decrease in temperature and during expansion the mixing process was faster, which led to the mixing of high and low temperature areas in the combustion chamber. Nitrogen decomposition stopped when the high temperature points inside the cylinder disappeared.

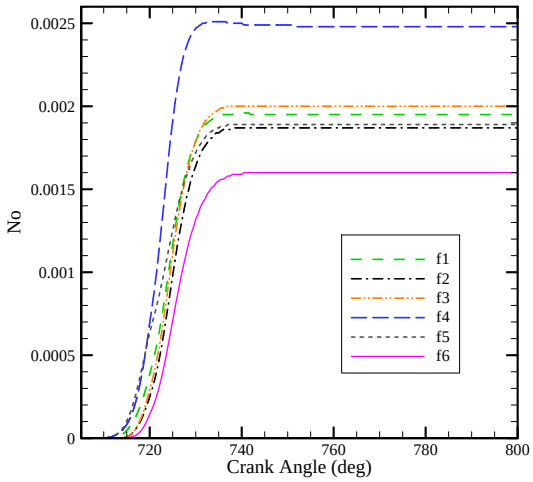

Fig. 11: NO variations for different injection patterns

Comparing nitrogen oxide changes for the first function in Fig. 11 with Fig. 6, one can conclude that the use of annular injector in the Kubota 3300 engine increased NO production in this engine. This is due to the fact that by improving the combustion performance of the engine using an annular injector in the Kubota engine, the temperature and pressure of the combustion chamber also increased and caused more nitrogen decomposition in the combustion chamber. Although the annular injector increased engine performance, this type of injector would generate more pollutants if nitrogen oxide absorbers were not used in the engine outlet. The highest average temperature was related to the fourth function, which was seen to have the highest nitrogen oxide production. On the other hand, the lowest temperature was related to the sixth function, which also had the lowest nitrogen oxide production for this function.

Fig. 12 shows the mass fraction of soot in terms of crankshaft angle. It can be seen that with the beginning of combustion and the rise of the chamber temperature, soot fraction increased due to the acceleration of reactions and shortage of oxygen supply to the combustible fuel. When the main combustion process was completed, due to the slowing down of the chemical reactions as well as the appropriate temperature and intensity of turbulence created inside the cylinder, the produced soot was oxidized and reduced. That is, over time, as the flame progressed inside the chamber, soot oxidation began, and the carbon

molecules combined with oxygen that was then delivered to them. In all the functions used for spraying, the soot was well oxidized and eliminated at the end. Therefore, the use of the annular injector in the Kubota 3300 engine does not cause any problems in terms of soot pollution.

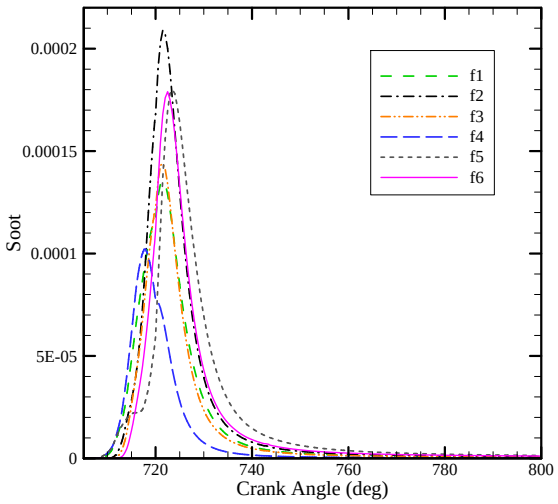

Fig. 12: Soot mass fraction variations for different injection patterns

Figs 13 to 16 demonstrate the distribution of some parameters at TDC and 40° aTDC for the sixth function. Fig. 13 shows the temperature distribution in combustion chamber. As it can be seen, the combustion starts from the central area, and gradually moves to the cylinder wall. At first the movement towards the wall was fast, but it was reduced with the expansion of the combustion chamber. Finally the parts of the high-temperature mixture were transferred to the central part. As demonstrated in Fig. 14, combustion occurs in areas with an equivalence ratio greater than 2.

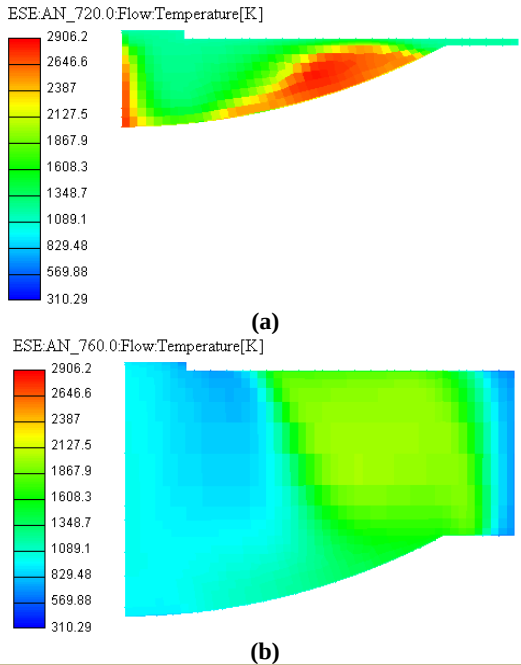

Fig. 13: Temperature distribution in combustion chamber: (a) at TDC, (b) at 40° aTDC

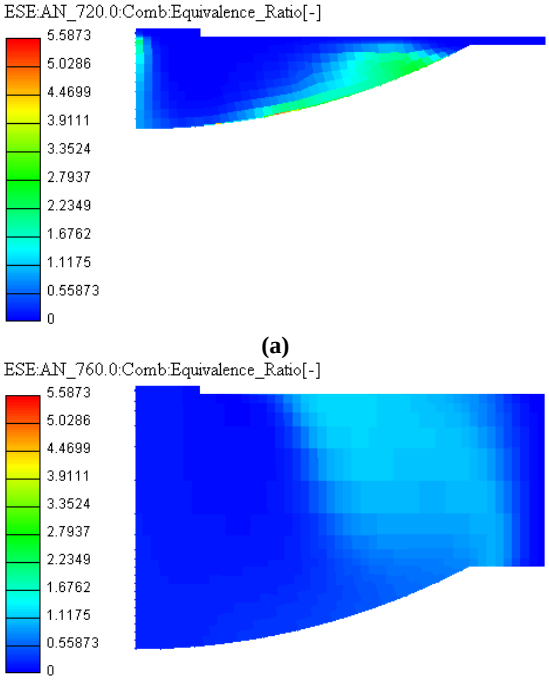

Fig. 14: Equivalence ratio distribution in combustion chamber: (a) at TDC, (b) at 40° aTDC

Fig. 15 shows nitrogen oxide distribution in the combustion chamber. It is that this pollutant is mostly produced at high temperature points. In areas with equivalence ratio of 1 and temperatures above 2000 K, NO has the highest mass fraction. Fig. 16 demonstrates distribution of soot in combustion chamber. Soot is produced in the area of the flame front and in oxygen-poor areas, where oxygen penetration rate into the combustion zone is not sufficient to reach stoichiometric conditions, which are closer to the piston crown. By comparing the distribution of soot in the two states of TDC and 40° aTDC, it can be seen that the soot produced at the beginning of combustion is well oxidized and eliminated at the end.

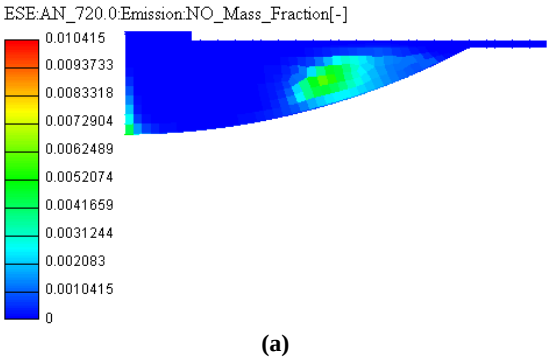

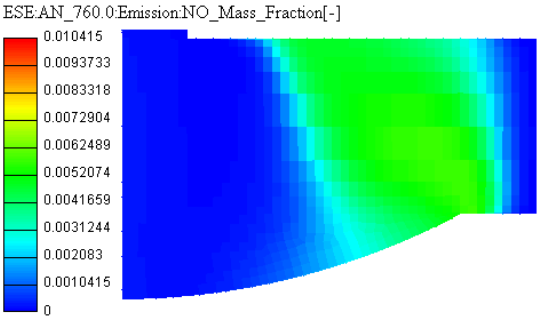

(b)

Fig. 15: NO distribution in combustion chamber: (a) at TDC, (b) at 40° aTDC

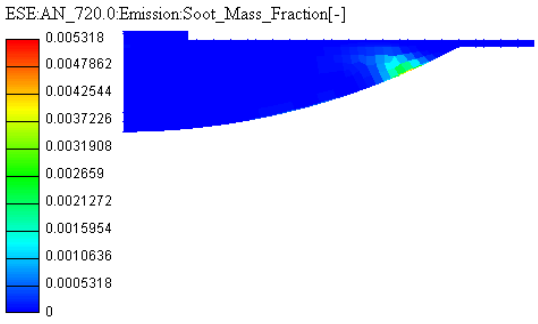

(a)

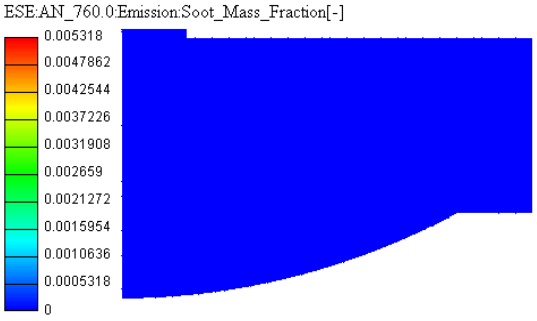

(b)

Fig. 16: Soot distribution in combustion chamber: (a) at TDC, (b) at 40° aTDC

Fig. 17 shows how fuel is sprayed into the combustion chamber. One of the features of annular injectors is increasing the angle of the spray cone, which the injector used in the present study has also done well. By careful investigation of the distributed droplets, it can be observed that the droplets diameter is close to each other, and they are distributed evenly from the central part to the edge of the spray cone. The simulation results show that controlling the penetration length of the fuel spray in the combustion chamber, increasing the angle of the spray cone, and, thus, the uniform distribution of fuel droplets are effective factors in proper combustion performance.

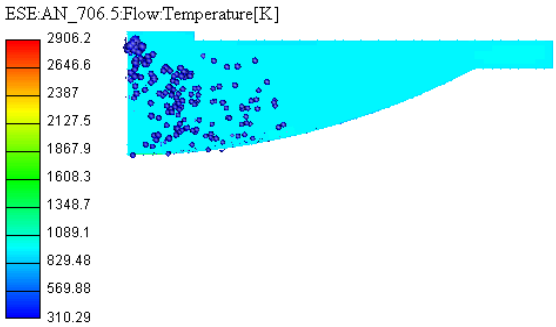

Fig. 17: Fuel spray into the combustion chamber

7. Conclusion

In the present study, the performance and emission production of Kubota 3300 engine using the presented annular injector and different diesel injection functions were studied numerically. Engine power, specific fuel consumption (SFC) and pollutants emission in the combustion chamber, using annular injector along with uniform mode and five different injection functions, were investigated. The results of fuel spray and engine performance simulations showed that the injector having annular orifice causes more uniform distribution of droplets and increases the spray cone angle. Using this type of injector led to a decrease in temperature at high temperature points inside the combustion chamber, which reduced nitrogen oxide emission. Moreover, increasing the cone angle without creating a very thin area by the annular injector created good balance between the production of nitrogen oxide and soot.

The results of numerical simulations also showed that the fuel injection function had great effect on engine performance and caused 5% difference between the SFC value for the first and the sixth function. Also, using different spray functions, without changing the spray length, changed the sprayed mass in each cycle, which resulted in 18% difference between the maximum (the fourth function) and the minimum (fifth function) of power. The sixth function had the best performance in terms of nitrogen oxide production, and nitrogen oxide fraction reached 0.0016. The use of annular injector in the Kubota 3300 engine and changing the sprayed mass increased soot mass at the beginning of the combustion process, but, then, the produced soot was oxidized well for all functions.

Nomenclature

A	constant, A=400
A	Zeldovich nitrogen oxide formation model constant
A_f	Hiroyasu soot formation model constant
B	constant, B=3
C_3	constant, C_3=1.17
C_{pr}	Empirical coefficient
C_{fu}	Empirical coefficient
D_s	soot particle diameter
d_{out}	orifice diameter
E_a	activation energy
h	sheet thickness in orifice
K_v	velocity coefficient
m_1	fluid mass rate

M_{fv}	fuel vapor mass
M_s	soot mass
MW_c	carbon molecular weight
$\ln\left(\frac{\eta}{\eta_0}\right)$	empirical dimensionless parameter
R_{tot}	reaction rate
P	pressure
ΔP	pressure difference
S	stoichiometric coefficient written on mass basis
SFC	specific fuel consumption
V	discharge absolute velocity
V_{rel}	discharge relative velocity
X	ratio of air core to the total area
y	mass fraction

Greek letters

μ	dynamic viscosity
τ_r	turbulent mixing time scale
ρ	fuel density
ρ_s	soot density
θ	half of the cone angle

References

[1] Kozina, A., Radica, G., Nižetić, S., "*Analysis of methods towards reduction of harmful pollutants from diesel engines*", Journal of Cleaner Production, Vol. 262, p.121105, July. 2020, https://doi: 10.1016/j.jclepro.2020.121105.

[2] Leach, F., Kalghatgi, G., Stone, R., Miles, P., "*The scope for improving the efficiency and environmental impact of internal combustion engines*", Transportation Engineering, Vol. 1, p.100005, June. 2020, https://doi:10.1016/j.treng.2020.100005.

[3] Mohan, B., Yang, W., kiang Chou, S., "*Fuel injection strategies for performance improvement and emissions reduction in compression ignition engines—A review*", Renewable and Sustainable Energy Reviews, Vol. 28, pp.664-676, December. 2013, https://doi:10.1016/j.rser.2013.08.051.

[4] Medina, M., Bautista, A., Wooldridge, M., Payri, R., "*The effects of injector geometry and operating conditions on spray mass, momentum and development using high-pressure gasoline*", Fuel, Vol. 294, p.120468, June. 2021, https://doi: 10.1016/j.fuel.2021.120468.

[5] Payri, R., Viera, J.P., Gopalakrishnan, V., Szymkowicz, P.G., "*The effect of nozzle geometry over the evaporative spray formation for three different fuels*", Fuel, Vol. 188, pp.645-660, January. 2017, https://doi: 10.1016/j.fuel.2016.10.064.

[6] Pulkrabek, W.W., *Engineering fundamentals of the internal combustion engine*, 2004.

[7] Zhang, Y., Nishida, K., Nomura, S., Ito, T., "*Spray characteristics of group-hole nozzle for D.I. diesel engine*", SAE Technical Paper Series, Oct. 2003, https://doi: 10.4271/2003-01-3115.

[8] Park, S.W., Suh, H.K., Lee, C.S., Abani, N., Reitz, R.D, "*Modeling of group-hole-nozzle sprays using grid-size-, hole-location-, and time-step-independent models*", Atomization and Sprays, Vol. 19, No. 6, pp. 567–582, Jan. 2009, https://doi: 10.1615/atomizspr.v19.i6.50.

[9] Park, S.W. and Reitz, R.D., "*Optimization of fuel/air mixture formation for stoichiometric diesel combustion using a 2-spray-angle group-hole nozzle*", Fuel, Vol. 88, No. 5, pp. 843–852, May 2009, https://doi: 10.1016/j.fuel.2008.10.028.

[10] Gao, J., Matsumoto, Y., Namba, M., Nishida, K., "*An investigation of mixture formation and in-cylinder combustion processes in direct injection diesel engines using group-hole nozzles*", International Journal of Engine Research, Vol. 10, No. 1, pp. 27–44, Feb. 2009, https://doi: 10.1243/14680874jer02108.

[11] Siebers, D., Higgins, B., "*Flame Lift-Off on Direct-Injection diesel sprays under quiescent conditions*", SAE Technical Paper Series, Mar. 2001, https://doi: 10.4271/2001-01-0530.

[12] Bergstrand, P., Försth, M., Denbratt, I., "*The influence of orifice diameter on flame lift-off length*", Zaragoza, Vol. 9, p.11, 2002.

[13] Yin, B., Xu, B., Jia, H., Yu, S., "*The Effect of Elliptical Diesel Nozzles on Spray Liquid-Phase Penetration under Evaporative Conditions*", Energies, Vol. 13, No. 9, p. 2234, May 2020, https://doi: 10.3390/en13092234.

[14] Sharma, P., Fang, T., "*Breakup of liquid jets from non-circular orifices*", Experiments in Fluids, Vol. 55, No. 2, Jan. 2014, https://doi: 10.1007/s00348-014-1666-z.

[15] Hashiehbaf, A., Romano, G.P., "*A phase averaged PIV study of circular and non-circular synthetic turbulent jets issuing from sharp edge orifices*", International Journal of Heat and Fluid Flow, Vol. 82, p. 108536, Apr. 2020, https://doi: 10.1016/j.ijheatfluidflow.2020.108536.

[16] Sharma, P., Fang, T., "*Spray and atomization of a common rail fuel injector with non-circular orifices*", Fuel, Vol. 153, pp. 416–430, Aug. 2015, https://doi: 10.1016/j.fuel.2015.02.119.

[17] Migliaccio, M., Montanaro, A., Beatrice, C., Napolitano, P., Allocca, L., Fraioli, V., "*Experimental and numerical analysis of a high-pressure outwardly opening hollow cone spray injector for automotive engines*", Fuel, Vol. 196, pp. 508–519, May 2017, https://doi: 10.1016/j.fuel.2017.01.020.

[18] Jeon, J., Moon, S., "*Ambient density effects on initial flow breakup and droplet size distribution of hollow-cone sprays from outwardly-opening GDI injector*", Fuel, Vol. 211, pp. 572–581, Jan. 2018, https://doi: 10.1016/j.fuel.2017.09.016.

[19] Gao, H., Zhang, F., Zhang, Z., Wang, E., Liu, B., "*Experimental investigation on the spray characteristic of air-assisted hollow-cone gasoline injector*", Applied Thermal Engineering, Vol. 151, pp. 354–363, Mar. 2019, https://doi: 10.1016/j.applthermaleng.2019.02.029.

[20] Du, J., Cenker, E., Badra, J., Sim, J., Roberts, W.L., "*Characteristics of a non-reacting spray from an outwardly opening hollow-cone injector with high-*

reactivity gasolines", Fuel, Vol. 268, p. 117293, May 2020, https://doi: 10.1016/j.fuel.2020.117293.

[21] Wu, H., Zhang, F., Zhang, Z., Gao, H., "*Experimental investigation on the spray characteristics of a self-pressurized hollow cone injector*", Fuel, Vol. 272, p. 117710, Jul. 2020, https://doi: 10.1016/j.fuel.2020.117710.

[22] Gimeno, J., Marti-Aldaravi, P., Carreres, M., Cardona, S., "*Experimental investigation of the lift-off height and soot formation of a spray flame for different co-flow conditions and fuels*", Combustion and Flame, Vol. 233, p. 111589, Nov. 2021, https://doi: 10.1016/j.combustflame.2021.111589.

[23] Soundararajan, P.R., Durox, D., Renaud, A., Vignat, G., Candel, S., "*Swirler effects on combustion instabilities analyzed with measured FDFs, injector impedances and damping rates*", Combustion and Flame, Vol. 238, p. 111947, Apr. 2022, https://doi: 10.1016/j.combustflame.2021.111947.

[24] Lee, C.S., Choi, N.J., "*Effect of air injection on the characteristics of transient response in a turbocharged diesel engine*", International Journal of Thermal Sciences, Vol. 41, No. 1, pp. 63–71, Jan. 2002, https://doi: 10.1016/s1290-0729(01)01304-7.

[25] Nishida, K., Zhang, W., Manabe, T., "*Effects of micro-hole and ultra-high injection pressure on mixture properties of DI diesel spray*", SAE Transactions, pp. 421-429, 2007.

[26] Celıkten, I., "*An experimental investigation of the effect of the injection pressure on engine performance and exhaust emission in indirect injection diesel engines*", Applied Thermal Engineering, Vol. 23, No. 16, pp. 2051–2060, Nov. 2003, https://doi: 10.1016/s1359-4311(03)00171-6.

[27] Das, P., Subbarao, P.M.V., Subrahmanyam, J.P., "*Control of combustion process in an HCCI-DI combustion engine using dual injection strategy with EGR*", Fuel, Vol. 159, pp. 580–589, Nov. 2015, https://doi: 10.1016/j.fuel.2015.07.009.

[28] Jeftić, M., Zheng, M., "*A study of the effect of post injection on combustion and emissions with premixing enhanced fueling strategies*", Applied Energy, Vol. 157, pp. 861–870, Nov. 2015, https://doi: 10.1016/j.apenergy.2015.02.052.

[29] Park, S.H., Yoon, S.H., "*Injection strategy for simultaneous reduction of NOx and soot emissions using two-stage injection in DME fueled engine*", Applied Energy, Vol. 143, pp. 262–270, Apr. 2015, https://doi: 10.1016/j.apenergy.2015.01.049.

[30] Macian, V., Payri, R., Ruiz, S., Bardi, M., Plazas, A.H., "*Experimental study of the relationship between injection rate shape and Diesel ignition using a novel piezo-actuated direct-acting injector*", Applied Energy, Vol. 118, pp. 100–113, Apr. 2014, https://doi: 10.1016/j.apenergy.2013.12.025.

[31] Mohan, B., Yang, W., Yu, W., Tay, K.L., Chou, S.K., "*Numerical investigation on the effects of injection rate shaping on combustion and emission characteristics of biodiesel fueled CI engine*", Applied Energy, Vol. 160, pp. 737–745, Dec. 2015, https://doi: 10.1016/j.apenergy.2015.08.034.

[32] Tay, K.L., Yang, W., Zhao, F., Yu, W., Mohan, B., "*A numerical study on the effects of boot injection rate-shapes on the combustion and emissions of a kerosene-diesel fueled direct injection compression ignition engine*", Fuel, Vol. 203, pp. 430–444, Sep. 2017, https://doi: 10.1016/j.fuel.2017.04.142.

[33] Wang, Z., Wyszynski, M.L., Xu, H., Abdullah, N.R., Piaszyk, J., "*Fuel injection and combustion study by the combination of mass flow rate and heat release rate with single and multiple injection strategies*", Fuel Processing Technology, Vol. 132, pp. 118–132, Apr. 2015, https://doi: 10.1016/j.fuproc.2014.11.024.

[34] Özkan, M., Özkan, D.B., Özener, O., Yılmaz, H., "*Experimental study on energy and exergy analyses of a diesel engine performed with multiple injection strategies: Effect of pre-injection timing*", Applied Thermal Engineering, Vol. 53, No. 1, pp. 21–30, Apr. 2013, https://doi: 10.1016/j.applthermaleng.2012.12.034.

[35] Roh, H.G., Lee, D., Lee, C.S., "*Impact of DME-biodiesel, diesel-biodiesel and diesel fuels on the combustion and emission reduction characteristics of a CI engine according to pilot and single injection strategies*", Journal of the Energy Institute, Vol. 88, No. 4, pp. 376–385, Nov. 2015, https://doi: 10.1016/j.joei.2014.11.005.

[36] Benajes, J., Molina, S., García, A., Monsalve-Serrano, J., Durrett, R., "*Performance and engine-out emissions evaluation of the double injection strategy applied to the gasoline partially premixed compression ignition spark assisted combustion concept*", Applied Energy, Vol. 134, pp. 90–101, Dec. 2014, https://doi: 10.1016/j.apenergy.2014.08.008.

[37] Jeon, J., Park, S., "*Effects of pilot injection strategies on the flame temperature and soot distributions in an optical CI engine fueled with biodiesel and conventional diesel*", Applied Energy, Vol. 160, pp. 581–591, Dec. 2015, https://doi: 10.1016/j.apenergy.2015.09.075.

[38] Lefebvre, A. H., McDonell, V.G., *Atomization and sprays*, 2017. https://doi: 10.1201/9781315120911.

[39] Clark, C.J., Dombrowski, N., "*Aerodynamic instability and disintegration of inviscid liquid sheets*", Proceedings of the Royal Society of London, Vol. 329, No. 1579, pp. 467–478, Sep. 1972, https://doi: 10.1098/rspa.1972.0124.

[40] Brink, A., Mueller, C., KILPINEN, P.A., Hupa, M., "*Possibilities and limitations of the eddy break-up model*", Combustion and flame, Vol. 123, No. 1-2, pp.275-279, 2000, https://doi:10.1016/S0010-2180(00)00146-2.

[41] Nishida, K., Hiroyasu, H., "*Simplified three-dimensional modeling of mixture formation and combustion in a DI diesel engine*", SAE transactions, pp.276-293, 1989.

[42] Dukowicz, J.K., "*A particle-fluid numerical model for liquid sprays*", Journal of Computational Physics, Vol. 35, No. 2, pp. 229–253, Apr. 1980, https://doi: 10.1016/0021-9991(80)90087-x.

[43] Hassan, N.M.S., Rasul, M.G., Harch, C.A., "*Modelling and experimental investigation of engine performance*

and emissions fuelled with biodiesel produced from Australian Beauty Leaf Tree", Fuel, Vol. 150, pp. 625–635, Jun. 2015, https://doi: 10.1016/j.fuel.2015.02.016.